Remote Sens. **2014**, *6*, 5238-5256; doi:10.3390/rs6065238

OPEN ACCESS

remote sensing

ISSN 2072-4292

www.mdpi.com/journal/remotesensing

Article

Comparison of Medium Spatial Resolution ENVISAT-MERIS and Terra-MODIS Time Series for Vegetation Decline Analysis: A Case Study in Central Asia

Julia Tüshaus [1,*], Olena Dubovyk [1,2], Asia Khamzina [3] and Gunter Menz [1,4]

[1] Center for Remote Sensing of Land Surfaces (ZFL), University of Bonn, Walter-Flex Str. 3, Bonn 53113, Germany; E-Mails: odubovyk@uni-bonn.de (O.D.); g.menz@uni-bonn.de (G.M.)

[2] Institute of Crop Science and Resource Conservation (INRES), University of Bonn, Katzenburgweg 5, Bonn 53115, Germany

[3] Center for Development Research (ZEF), University of Bonn, Walter-Flex Str. 3, Bonn 53113, Germany; E-Mail: asia.khamzina@uni-bonn.de

[4] Remote Sensing Research Group, Department of Geography, University of Bonn, Meckenheimer Allee 166, Bonn 53115, Germany

***** Author to whom correspondence should be addressed; E-Mail: julia.tueshaus@uni-bonn.de; Tel.: +49-228-73-4925; Fax: +49-228-73-6857.

Received: 2 October 2013; in revised form: 30 May 2014 / Accepted: 30 May 2014 / Published: 6 June 2014

Abstract: Accurate monitoring of land surface dynamics using remote sensing is essential for the synoptic assessment of environmental change. We assessed a Medium Resolution Imaging Spectrometer (MERIS) full resolution dataset for vegetation monitoring as an alternative to the more commonly used Moderate-Resolution Imaging Spectroradiometer (MODIS) data. Time series of vegetation indices calculated from 300 m resolution MERIS and 250 m resolution MODIS datasets were analyzed to monitor vegetation productivity trends in the irrigated lowlands in Northern Uzbekistan for the period 2003–2011. Mann-Kendall trend analysis was conducted using the time series of Normalized Differenced Vegetation Index (NDVI), Soil-Adjusted Vegetation Index (SAVI), and MERIS-based Terrestrial Chlorophyll Index (MTCI) to detect trends and examine the capabilities of each sensor and index. The methodology consisted of (1) preprocessing of the original imagery; (2) processing and statistical analysis of the corresponding time series datasets; and (3) comparison of the resulting trends. Results confirmed the occurrence of widespread vegetation productivity decline, ranging from 5.5% (MERIS-MTCI) to 21% (MODIS-NDVI) of the total irrigated cropland in the study area. All indices identified

the same spatial patterns of decreasing vegetation. Average vegetation index values of NDVI and SAVI were slightly higher when measured by MERIS than by MODIS. These differences merit further investigation to allow a fusion of these datasets for consistent monitoring of cropland productivity decline at scales suitable for guiding operational land management practices.

Keywords: time series analysis; vegetation productivity; uzbekistan; vegetation indices; Mann-Kendall; irrigated cropland

1. Introduction

Land surface dynamics is one of the key drivers of global environmental change and earth observation is the most important tool for its monitoring [1]. Remote sensing based land dynamics monitoring relies on a wide range of change detection methods [2,3]. One set of such techniques utilizes image classification to derive multi-temporal land use/land cover (LULC) maps. These maps are then compared to identify changes in mapped classes [4–6]. Applicability of these methods depends on availability of training data and accuracies of prior classifications [7]. Classification-based analyses are limited in that they do not allow evaluation of subtle changes within single classes. These changes are important in a number of environmental applications, including land degradation monitoring. Such gradual change can be effectively captured by applying algorithms (e.g., regression analyses) that measure spectral differences among image acquisition dates [8–10].

Trend analyses of time series satellite data are well-suited for land surface dynamics monitoring [1] and have been routinely applied using coarse-scale imagery [9,11]. However, imagery acquired by medium spatial resolution sensors including AQUA/TERRA Moderate-Resolution Imaging Spectroradiometer (MODIS) and ENVISAT Medium Resolution Imaging Spectrometer (MERIS) have been of less utility in such analyses due to their relatively shorter data archives. Additionally, coarse resolution sensors fail to generate image information at the spatial levels required for environmental management at landscape scale. Thus, medium- to high-resolution imagery is essential for such analyses [12,13].

Currently, a debate is ongoing regarding the choice of vegetation indices (VIs) to monitor gradual vegetation changes using satellite time series [1,14]. The Normalized Differenced Vegetation Index (NDVI) is the most commonly used indicator for vegetation productivity monitoring [15,16]. However, NDVI has some well-documented limitations, including saturation at high levels of vegetation biomass and chlorophyll concentration [17] and a sensitivity to changing atmospheric conditions [18]. For example, a study demonstrated that NDVI was not a very robust proxy for biomass monitoring in semi-arid Senegal [19]. The MERIS Terrestrial Chlorophyll Index (MTCI) [20] and the Soil-Adjusted Vegetation Index (SAVI) [21] were designed to reduce sensitivity to atmospheric effects, view angle, and soil background reflectance. Medium resolution VIs time series trend analyses play an important role in vegetation monitoring but a quantitative comparison of trend analysis results based on choice of VIs is lacking [1].

Relatively little attention has been paid to the differences in the trends calculated utilizing data acquired from different sensors. The results of VIs-based regression analysis due to the choice of the sensor were compared using coarse resolution satellite time series. A comparison of the linear NDVI trends calculated from 1-km AVHRR (Advanced Very High Resolution Radiometer), MODIS and SPOT Vegetation (Satellite Pour l'Observation de la Terre) time series showed distinct differences among NDVI trends derived from these sensors [22]. Additional studies have documented similarities but also disagreements between coarse resolution AVHRR-NDVI and MODIS-NDVI. Weaker correlations have been shown between these two datasets when applied in sparsely vegetated regions, such as Central Asia [23,24]. These differences in the results of trend analyses using medium resolution time series from MODIS and MERIS remain a topic for further research.

The MODIS and MERIS sensors have similar spatial and temporal resolutions, but MERIS has spectral characteristics that are better suited for interpreting vegetation parameters [25]. Atmospheric and soil influences are reduced for specific MERIS indices such as MTCI [20]. Several studies using MERIS-based VIs have been conducted [26–29]. For example, an evaluation of a time series of VIs derived from MODIS, MERIS, and SPOT imagery acquired during 2003 covering a semiarid natural grass savanna in Senegal was performed [30]. This study demonstrated that MERIS- and MODIS-derived indices produced reliable results for vegetation monitoring, but these indices did not document vegetation trends in the study area. In a related study, an MTCI time series (with 4.6 km spatial resolution) was also analyzed to detect phenological trends in India during the period of 2003–2007 [31]. These studies confirm MERIS as a useful sensor for assessing vegetation trends. To date, however, no study has applied a decade-long full resolution (300 m) MERIS time series for analyses and comparison of vegetation trends. Thus, the opportunity remains to study the 300 m MERIS-based VIs trends and to compare and contrast results between 300 m MERIS-VIs time series with those derived from other, similar sensors (including the 250 m MODIS sensor). The results of such analyses are essential to allow researchers to integrate different datasets for consistent vegetation trend monitoring. The Ocean and Land Color Instrument (OLCI) aboard the upcoming ESA-Sentinel-3 mission will continue MERIS measurements. It is therefore important to go on with investigating MERIS capabilities to help assure data continuity and to encoure the use of OLCI data also for land applications.

The goals of our study included calculation of VIs-based trends from the 300 m MERIS and 250 m MODIS time series and comparison of the resulting trends based on the different indices and sensors over the study area. Our study area focused on irrigated croplands in Uzbekistan. Due to irrigation inputs and suboptimal performance of drainage-collector systems, more than 50% of the irrigated land in the country is affected by soil salinization and waterlogging. These factors threaten cropland productivity. In this context, appropriate monitoring of long-term changes in cropland vegetation cover through remote sensing is an important prerequisite for the sustainable land management [32].

2. Study Area

Our study area is located in the lower Amu Darya River Basin in Northern Uzbekistan and covers irrigated croplands of the Khorezm region and southern part of the Autonomous Republic of Karakalpakstan (Figure 1). The total area of Khorezm and Southern Karakalpakstan is 854,500 ha, with irrigated cropland occupying approximately 410,000 ha [33]. The study area is characterized by

an extremely arid, continental climate. The annual average air temperature is 13.4 ℃ with seasonal temperatures ranging between 40 ℃ in summer to freezing in winter. Average precipitation totals approximately 100 mm per year and occurs mostly outside the April-October crop growing season. Crop cultivation therefore is entirely dependant on irrigation, with the Amu Darya River as the principal water source [34].

Figure 1. Location map of the study area in Uzbekistan.

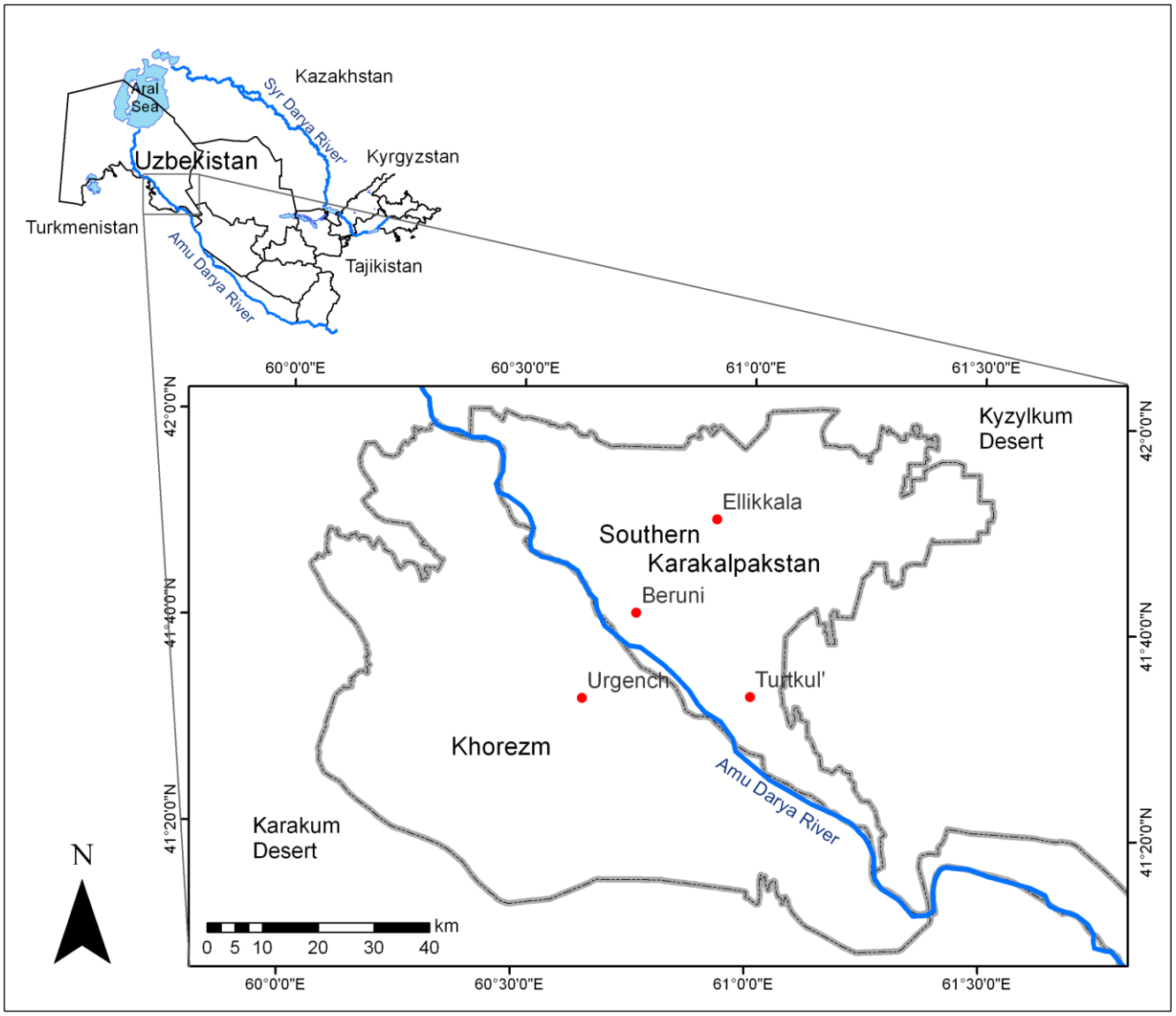

The major crops are cotton and winter wheat grown on up to 60% and 30% of the cropland, respectively [35]. The cotton and winter wheat cropping pattern is regulated by the state policy that defines cultivation areas for cotton and yield targets for both crops [36]. Land degradation in the form of secondary soil salinization is particularly widespread in these lowland areas, mainly due to inefficient irrigation and drainage practices which cause a rise in groundwater tables and threaten crop yields [37,38].

3. Methods and Material

3.1. Satellite Imagery

Time series of MERIS and MODIS imagery were used in this study. This data set covered the principal May-September annual crop growing season for the 2003–2011 period. MERIS full resolution data (300 m) at level 2 (MERIS_FR_2P) with a temporal resolution of 3 days were used for the analysis. Level 2 MERIS data are specified as *top of aerosol reflectance data* and have been systematically corrected for gaseous absorption, Rayleigh atmospheric scattering, water vapor absorption and ozone correction [39]. MER_FR_2P imagery is not per se corrected for angular effects over land and is therefore influenced by this within its 68.5 ° field of view. Directionality is however accounted for when the correction for a molecular scattering contribution is done for this product to derive reflectance over land surfaces [39]. MODIS MOD09Q1 Level 3 products have a spatial resolution of 250 m and display corrected ground-level surface spectral reflectance without atmospheric scattering and absorption. MOD09Q1 images are 8-day composites, containing only optimal available pixel-based reflectances from an 8-day period [40]. The study area is located close to the nadir line of MODIS and MERIS with a viewing angle within 10–20 °, which minimizes angular effects.

3.2. Methods

Drylands degradation is principally manifested in the reduced productive potential of the land [41], and may be detected via declined vegetation productivity over time. Vegetation growth per unit area and time is used as the basis for remote sensing-based land productivity assessments [42]. In dryland environments, the results of summing VIs, such as NDVI and SAVI, over a growing season are strongly correlated with vegetation productivity [43]. Using trend analysis of VIs time series, negative changes in VIs can be detected and further related to negative changes in vegetation productivity and degradation [44]. In irrigated agricultural environments, crop growth is adversely affected by soil salinization due to inefficient salt leaching and drainage [45], which leads to yield decline. In drought years, farmers tend to limit crop cultivation to areas with most fertile soil [13], which also cause decline in cropland vegetation cover. Regardless if induced by soil salinization or reduced cultivation, a continuous loss of cropland vegetation indicates the degradation of the cropland productive value [13].

Our methodology in this study consisted of several steps: (1) preprocessing of the original MERIS and MODIS images; (2) statistical analysis of the corresponding time series datasets; and (3) comparison of the resulting trends.

Image preprocessing included masking of clouds and invalid reflectances flagged by ESA (MERIS) and NASA (MODIS) preprocessing. Three different VIs were used in this study. MTCI is claimed to be a useful indicator for enhanced vegetation monitoring. This VI (Equation (1) [20]) uses data in three red/NIR spectral bands, including a red edge band (Table 1). MTCI was evaluated using model outputs, *in situ* field observations and MERIS data. This evaluation suggested MTCI sensitivity to high levels of chlorophyll content along with limited sensitivities to spatial resolution or atmospheric effects [46]. MTCI includes Band 9, located in the red-edge region related to chlorophyll content and vegetation productivity [47]. NDVI is a well understood and commonly used vegetation index associated with vegetation productivity (Equation (2) [48]; Table 1). Probably best described as

relative measure of vegetation vigor and photosynthetic activity, NDVI has been correlated with such physical measurements as total standing biomass, green leaf-area index (LAI) and percent of vegetation cover [49]. It is most often used among other applications as a tool for monitoring temporal changes in vegetation. However, NDVI is affected by soil spectral properties, specifically in environments of sparse vegetation. This may lead to underestimation of vegetation on bright soils or to overestimation of vegetation on dark soils [50]. To compensate for these drawbacks, several alternative VIs have been developed. For this study we utilized SAVI, an index that is based on the soil-line concept to reduce sensitivity to the soil background influences [21]. Technically, SAVI is a refinement of NDVI that incorporates an additive term *L* to correct for the soil background influence (Equation (3) [21]; Table 1).

$$\mathrm{MTCI} = \frac{\rho_{\mathrm{nir}} - \rho_{\mathrm{red\ edge}}}{\rho_{\mathrm{red\ edge}} - \rho_{\mathrm{red}}} \quad (1)$$

$$\mathrm{NDVI} = \frac{\rho_{\mathrm{nir}} - \rho_{\mathrm{red}}}{\rho_{\mathrm{nir}} + \rho_{\mathrm{red}}} \quad (2)$$

$$\mathrm{SAVI} = \frac{\rho_{\mathrm{nir}} - \rho_{\mathrm{red}}}{\rho_{nir} + \rho_{\mathrm{red}} + \mathrm{L}} (1 + \mathrm{L}) \quad (3)$$

where ρ = reflectance; nir = near infrared; L = soil adjustment factor (in this case L = 0.5).

Table 1. Bands of Medium Resolution Imaging Spectrometer (MERIS) and Moderate-Resolution Imaging Spectroradiometer (MODIS) used for the calculation of vegetation indices.

Spectrum	MERIS-MTCI	MERIS-NDVI/SAVI	MODIS-NDVI/SAVI
red	band 8 (677.5–685 nm)	band 7 (660–670 nm)	band 1 (620–670 nm)
nir	band 10 (750–757.5 nm)	band 13 (855–875 nm)	band 2 (841–876 nm)
red edge	band 9 (703.75–713.75 nm)	-	-

All images were co-registered to allow a correct pixel-by-pixel analysis [51]. Subsequently, all single MERIS-based VI images were temporally composited. A Maximum Value Composite (MVC) was used to reduce cloud influence, atmospheric effects, and surface directional reflectances [52].

The different time series were further preprocessed by denoising and deseasoning. Temporal denoising removes unexplained remaining noise from the image series by smoothing the curve over time [53]. Such noise includes spectral outliers caused by clouds and soil or sensor miscalibration. A mean filter was then applied using a symmetric moving window over the entire image series. The filter length variable was set to 3, utilizing three subsequent images to derive a smoothed mean value for each pixel. Deseasoning is an important process to account for spectral variances present within the image set due to vegetation seasonality. A common method to remove seasonality from the time series calculates sums of each VI per pixel for each growing season. In this way, trends that occur throughout the monitoring period can be detected [54].

Mann-Kendall trend analysis was conducted on the processed time series [55,56]. This method is a non-parametric trend test which estimates the presence of a monotonic single direction trend in the time series and is often used in vegetation studies [57,58]. The Kendall's correlation coefficient *Tau* ranges from −1 to +1; *Tau* values of −1 and +1 indicate consistent negative and positive trends

while a 0 value indicates no trend. The statistical significance of the trends was assessed by calculating the probability of a random trend for every pixel. Furthermore, the robustness of the trends was tested by adding an artificial outlier to the time series [58].

To compare the results from MERIS and MODIS vegetation trends, MERIS images were resampled to MODIS 250-m resolution using a Nearest Neighbor method. Temporal profiles and trend maps of all time series were first compared visually. For quantitative comparisons of different indices of the same sensor, a pixel-wise linear regression was conducted employing a deseasoned time series, as well as the Mann-Kendall *Tau* data [24,59]. Because the separate MERIS and MODIS datasets were used to measure the same parameter (VIs), it was necessary to evaluate the relative agreement between the identical VIs derived from the two different sensors. Bland-Altman-plots [60] were employed for this task. Correspondence between the two "methods" of deriving the same parameter was assessed by comparing the differences of these two datasets with their mean values. The image processing conducted in this study likely minimized the impact of the angular effects, because vegetation trends and not only the whole vegetation time series were compared between MERIS and MODIS. Calculated VI trends reflect relative changes in reflectances rather than their absolute values and, thus, allow a comparison between the two sensors [61].

Finally, in order to account for scale effects resulting from the different spatial resolution of MERIS and MODIS imagery, trend analysis was also conducted utilizing a second derived dataset. This dataset was compiled by rescaling the images to 1500 m resolution through integration of 5×5 MERIS pixels and 6×6 MODIS pixels. Trend analysis and comparison was then conducted on these datasets.

4. Results and Discussion

4.1. Vegetation Productivity Decline in the Study Area

MERIS- and MODIS-based trend maps produced in this study document distinct negative vegetation trends in the study area (Figure 2a–e; Table 2). These trends indicate a decline in cropland productivity that has also been described in earlier regional studies [13,33]. Negative vegetation trends dominated in the southwest of the Khorezm region that borders on the Karakum Desert and in the northwest and northeast parts of the study area adjacent to the Kyzylkum Desert. Several smaller areas of negative vegetation trend were also identified throughout the study area.

Areal statistics and single trend maps show that the spatial distribution of statistically significant negative trends varied depending on the sensor and choice of VI. Each of the five trend maps detected clusters of significant negative trends in the southwest and northern sections of the study region. These areas are predominantly of low soil quality and are also characterized by low population density [33]. Areas of significant negative trends ranged in size from 22,472 ha (MERIS-MTCI) to 85,510 ha (MODIS-NDVI); or between 5.5% and 20.1% of the irrigated cropland in the study area (Table 2). Results of the 1500 m resolution time series showed similar spatial distribution patterns of the trends, although the total area affected by negative trends based on NDVI is larger for both sensors due to 1500 m pixel size (Table 2). This underlines the applied value of using medium spatial resolution satellite imagery for land management applications.

Figure 2. Vegetation trend maps calculated from full resolution 2003–2011 time-series of (**a**) MERIS-NDVI; (**b**) MERIS-SAVI; (**c**) MERIS-MTCI; (**d**) MODIS-NDVI; and (**e**) MODIS-SAVI. Only significant negative trends ($p < 0.1$) are shown.

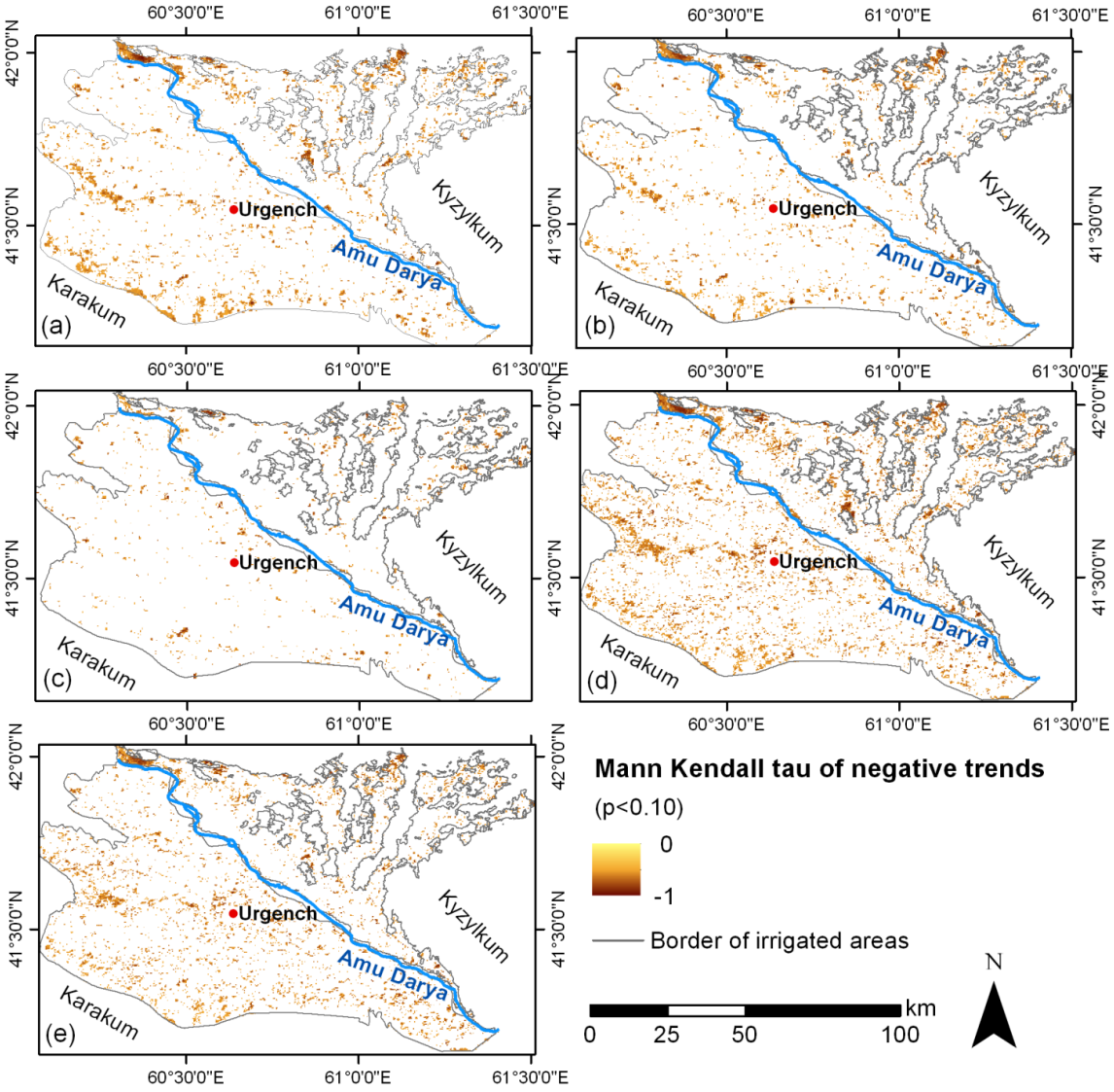

Table 2. Areal statistics of significant negative vegetation trends ($p < 0.1$) based on full resolution MERIS and MODIS vegetation indices. For comparison, data based on 1500 m resolution imagery are presented in brackets.

Vegetation Index	MERIS			MODIS		
	ha	% of Study Area	% of Irrigated Land	ha	% of Study Area	% of Irrigated Land
NDVI	57,724.02 (66,774.50)	6.8 (7.8)	14.1 (16.3)	85,509.82 (126,079.78)	10.0 (14.8)	20.1 (30.8)
SAVI	43,826.66 (43,836.65)	5.1 (5.1)	10.7 (10.7)	60,537.16 (72,469.40)	7.1 (8.5)	14.8 (17.7)
MTCI	22,472.32 (20,352.45)	2.6 (2.4)	5.5 (5.0)	-	-	-

Similar regional vegetation trends were observed by Dubovyk *et al.* (2013) [33]. In this analysis, cropland productivity decline in the same study area was documented for the period of 2000–2010 by linear trend analysis using 16-day 250 m MODIS-NDVI data. Significant negative vegetation trends were identified in 23% (94,835 ha) of the irrigated area in the study region. This result is directly comparable to the 20% value (85,510 ha) calculated in our current study derived using 250 m MODIS-NDVI time series.

4.2. Comparison of Time Series and Trends

4.2.1. Vegetation Index Time Series

For MERIS- and MODIS-based trend analyses, NDVI time series identified an area of significant negative trends up to 1.5 times larger than SAVI time series. SAVI has been found to be more appropriate for the detection of bare soil patches that are more likely to succumb to erosion and degradation due to the loss of protective vegetation cover [21]. Pixel-wise linear regression of MERIS- and MODIS-NDVI and -SAVI time series were however highly correlated (Table 3).

Table 3. R^2 values calculated by linear regression between indices (averaged over the entire study area). For comparison, R^2 based on 1500 m resolution imagery is presented in brackets.

Linear Regression		R^2 of Time Series	R^2 of Trends
MERIS	NDVI *vs.* SAVI	0.90 (0.92)	0.84 (0.84)
MERIS	MTCI *vs.* NDVI	0.22 (0.18)	0.11 (0.07)
MERIS	MTCI *vs.* SAVI	0.25 (0.21)	0.17 (0.12)
MODIS	NDVI *vs.* SAVI	0.88 (0.86)	0.83 (0.76)

The spatial pattern of high correlation pixels reflected locations with strongest negative vegetation trend in the study area (Figure 3a,b). In addition, correlations between NDVI and SAVI Mann-Kendall *Tau* coefficients were high for both sensors (Table 3). The *Tau* values of NDVI (x-axis) and SAVI (y-axis) were distributed almost linearly, with narrower relations observed at very low and very high trend values (Figure 4a,b). The correlation between NDVI and SAVI was high because both indices are derived by the same combination of spectral reflectance bands. MERIS-MTCI time series data as well as trend values exhibited low correlations with MERIS-NDVI and SAVI (Figure 3c, Figure 4c, and Table 3). Comparison of trends based on 1500 m time series showed quite similar results (Table 3).

Differences between MTCI and NDVI were also found. MTCI images showed higher spatial variations of vegetation status than NDVI, specifically in regions with a high vegetation chlorophyll content [20]. The low correlation between NDVI and MTCI may be rooted in the relationship of MTCI to vegetation chlorophyll content. While NDVI and SAVI are related to biomass and vegetation cover that saturate at high levels [31], MTCI has a limited ability to identify vegetation status in areas of sparse vegetation cover. These areas dominate the degraded cropland in the study region. Lower *Tau* values may also be related to influences of canopy structure on MTCI retrieval. MTCI values are often overestimated within barren land enviromnents [62]. MTCI trend analysis was able to identify fewer negative vegetation trend pixels located within areas of sparse vegetation cover. Our results support the

fundamental conclusion that NDVI overestimates negative vegetation trends while MTCI underestimates these trends.

Figure 3. Pixel-wise R^2 between full resolution time series of (**a**) MERIS-NDVI and -SAVI; (**b**) MERIS-NDVI and -MTCI; (**c**) MODIS-NDVI and -SAVI; (**d**) MERIS- and MODIS-NDVI; and (**e**) MERIS- and MODIS-SAVI.

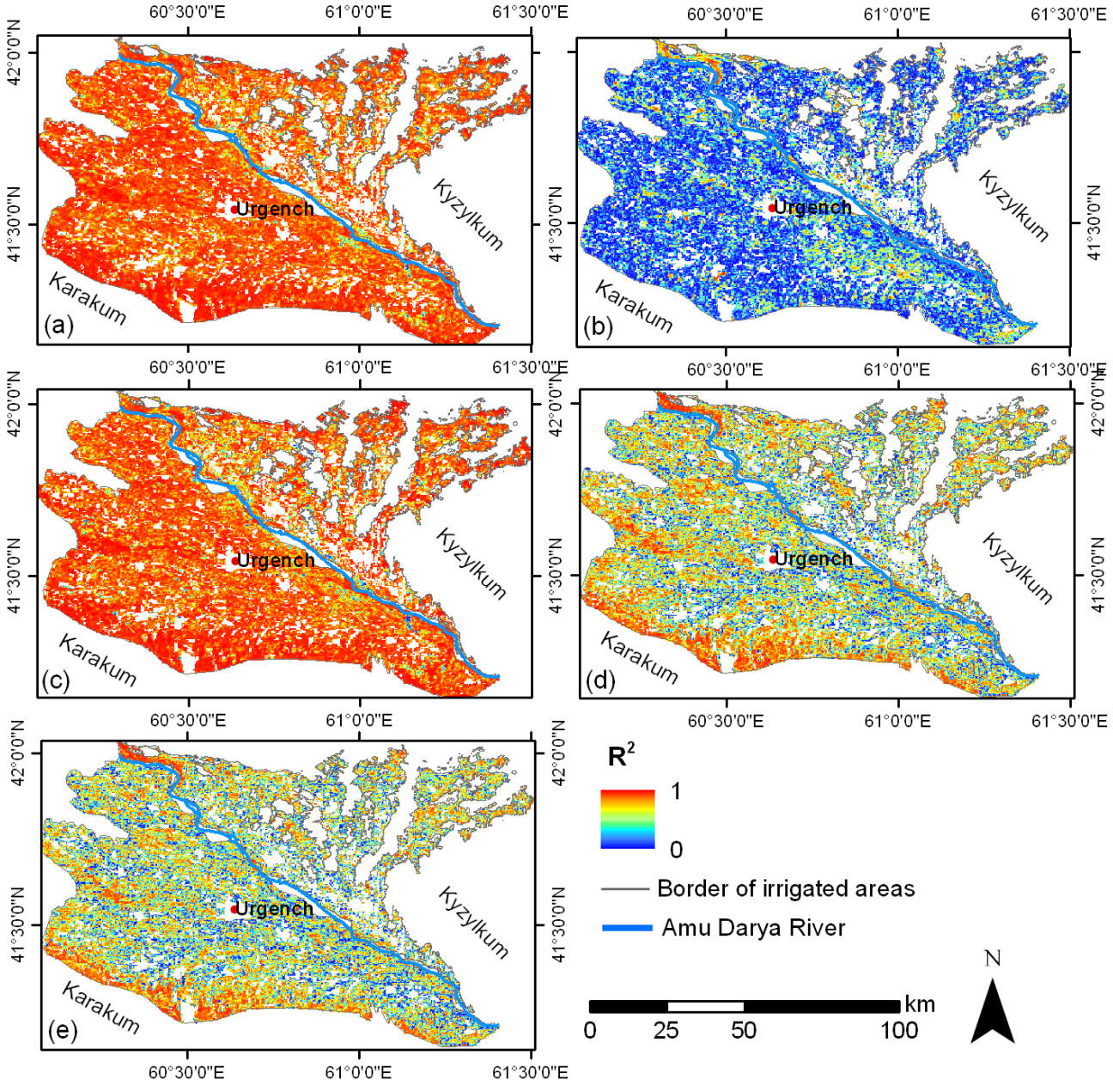

The temporal profiles of both MERIS- and MODIS-NDVI and -SAVI time series reflect the seasonal vegetation cycle, with maximum values for both time series occuring during mid- and late August (Figure 5a). The seasonal profile based on MERIS-MTCI (Figure 5b) showed two distinctive maxima in each year as well as large fluctuations of MTCI values from one time step to another. The first peak may refer to the maturation of winter wheat, harvested in June, while the second may refer to cotton, harvested in September-October. NDVI and SAVI only marginally reflect these two different crop phases because they detect vegetation cover which may not be affected

strongly by the harvest of winter wheat as cotton is already in its budding phase in June. Therefore, MTCI may be more suitable for the assessment of the crop phenology rather than vegetation productivity [18]. All of the time series showed lower greenness in 2008 and 2011 than in the other years, most probably due to the droughts that occurred in these two years [63].

Figure 4. Scatterplots of Mann-Kendall *Tau* trends based on (**a**) MERIS-NDVI and -SAVI; (**b**) MODIS-NDVI and -SAVI; and (**c**) MERIS-NDVI and -MTCI time series.

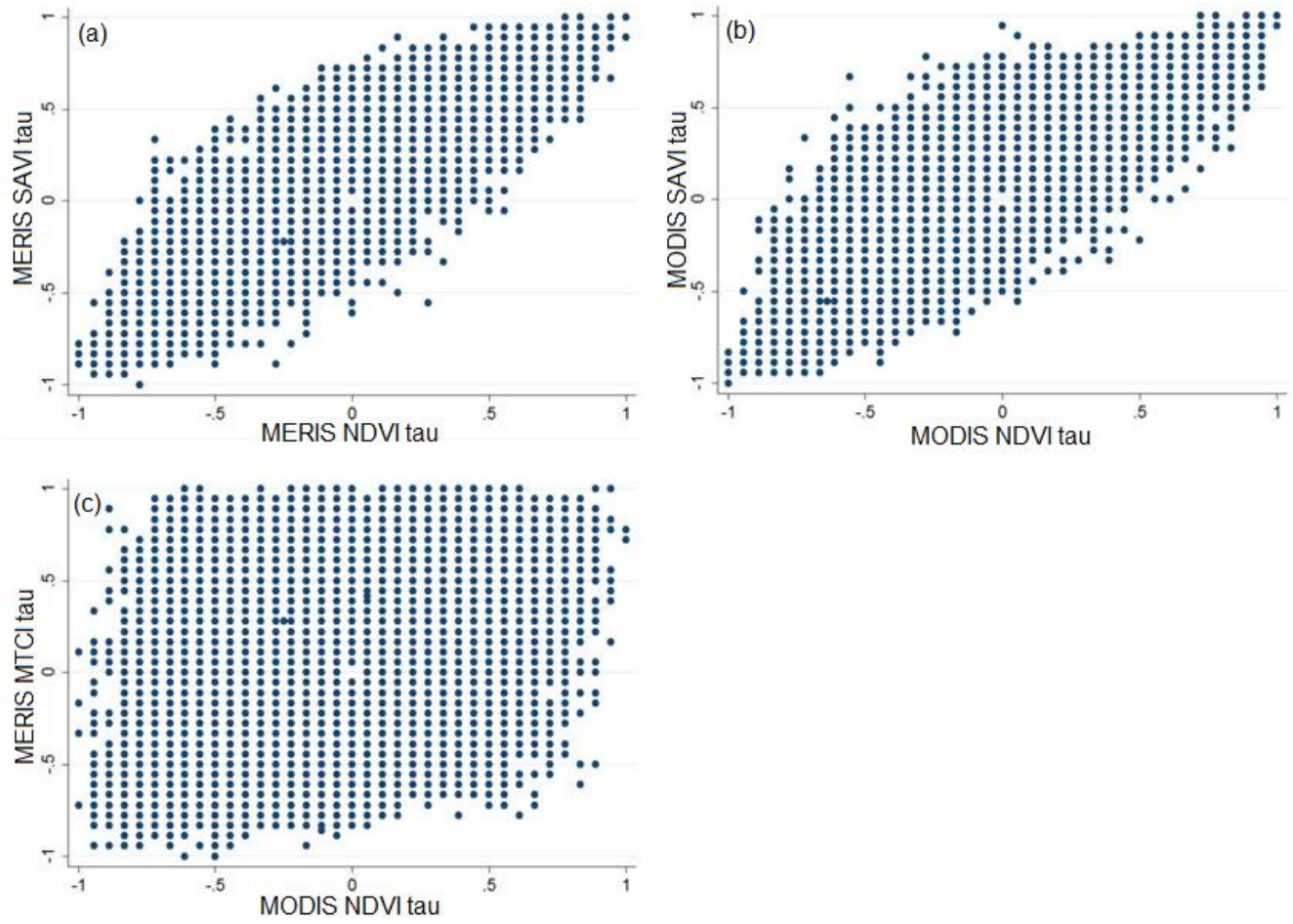

Figure 5. Temporal profiles of (**a**) filtered MERIS- and MODIS-NDVI and -SAVI and (**b**) MERIS-MTCI full resolution time series for each growing season from 2003 to 2011. Indices are averaged over the entire study area.

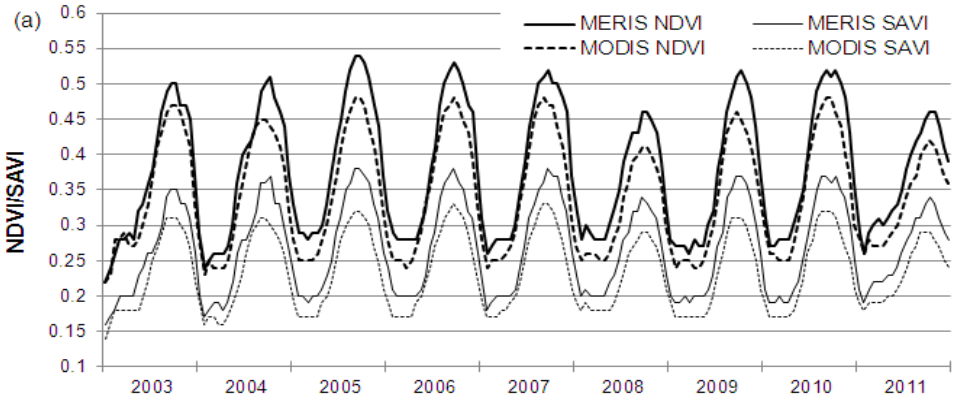

Figure 5. *Cont.*

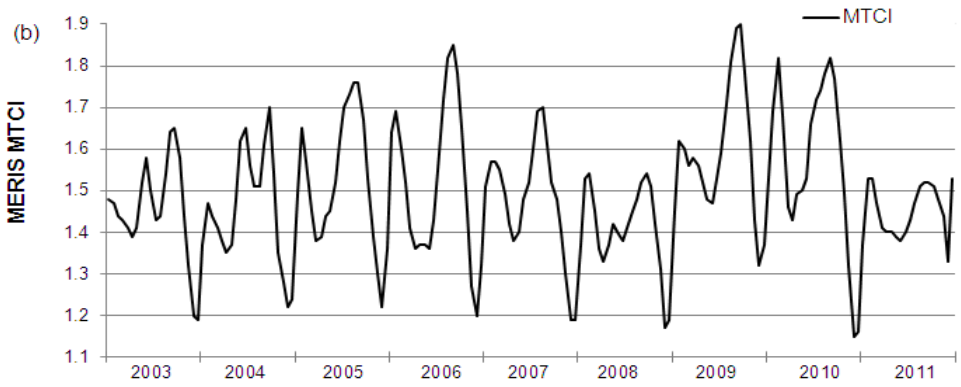

4.2.2. MERIS and MODIS Time Series and Trends

Generally, both MERIS- and MODIS-NDVI and -SAVI trends revealed the same clusters of vegetation productivity decline. However, the results showed that average vegetation values were higher when measured by MERIS than by MODIS, especially at the maxima and minima of each growing season. Specifically, MODIS-NDVI and -SAVI trend analyses showed nearly 1.5 times larger areas of negative trends than MERIS (Table 2). Pixel-wise linear regression revealed high correlation zones between MODIS and MERIS based NDVI time series clustered at the borders to the deserts in the north and the south, as well as in an east/west oriented zone located west of the city of Urgench in the Khorezm region. Negative vegetation trends were also observed in these regions, indicating spatial differentiation of the correlation between MODIS and MERIS time series (Figure 3d,e). However, agreement between MERIS and MODIS was higher where Mann-Kendall *Tau* trends were strong (as values approached −1 and 1) and lower where these trends were less pronounced (between values of −0.6 and 0.6; see Figure 6a,b). We attribute this to strong temporal vegetation status variations between MERIS and MODIS, or to external factors which may influence reflectances, such as changes in cropping patterns.

Figure 6. Bland-Altman plots of (**a**) MODIS- and MERIS-NDVI and (**b**) MODIS- and MERIS-SAVI presenting the difference (y-axis) against average vegetation values (x-axis). The grey area marks the region where values agree significantly, while the vertical dashed lines visualize the separation of the very low and very high mean values with low differences.

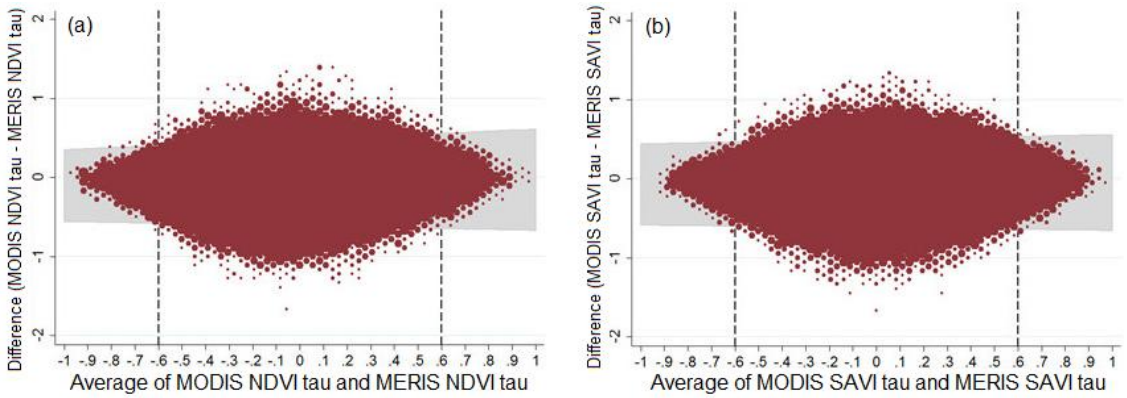

In addition to environmental factors, internal MERIS and MODIS sensor and preprocessing differences may lead to discrepancies in results [30]. MERIS and MODIS imagery have spatial resolutions of 300 m and 250 m, respectively. Thus, a more diverse mix of land cover may be present in MERIS image pixels than in MODIS imagery, resulting in differing spectral reflectance values for individual pixels. The differing spatial resolution of the image sets also complicated the pixel-wise comparison of trend images. However, the analysis of a second dataset of 1500 m resolution showed that this effect was relatively small in our case. Absolute geolocation accuracy of the data sets also must be considered; while MERIS images were reprojected and co-registered, inaccuracies cannot be excluded [25,51]. Differing sensor spectral resolution characteristics may also be a factor in the observed discrepancies. MODIS spectral bands are generally wider than MERIS bands and the center location of each band is also shifted [64,65]. Viewing effects, gridding artifacts and differences in atmospheric correction procedures may all be factors in the divergence of observed results [51]. Especially viewing effects, *i.e.*, directional reflectances caused by different sun zenith angle, sun azimuth angle and view zenith angle, may influence the VI values of MERIS and MODIS [66]. Although preprocessing steps, such as maximum value compositing and comparison of trends, are likely to reduce angular effects [52], a comparison of these effects between MODIS and MERIS is an important topic for a consequent study and could be addressed via radiative-transfer modeling or by using simple model based on BRDF parameters [61]. To enhance usability of both medium resolution datasets from MODIS and MERIS, either BRDF-correction should be inherently included in these products or operational automated tools for BRDF correction, which are currently not available, should be developed by the image providers.

The trend analysis/time series methodology itself also has some limitations for the detection of vegetation productivity decline [58]. Different methods applied on the same data may lead to contradictory results [57]. The temporal aspect of a particular productivity decline is also sinificant. The decline occuring at the beginning or end of the time series was often not detected by trend analysis, while the decline beginning in the middle of the time series typically was detected [58]. Furthermore, the rate of decline affects its detectability. A generally strong vegetation trend within an observation period may not be detected by Mann-Kendall trend analysis when yearly fluctuations are moderate [67].

All of the above issues mandated caution when vegetation productivity trends were interpreted for this study. They should likewise do so in general applications of MERIS time series for detecting negative vegetation trends in cropping systems. With these considerations in mind, it is still important to consider that trend analysis of satellite time series data is currently the only available means to independently monitor gradual vegetation changes through time. The obtained results also widen the scope for application of the trend analysis of time series of satellite images to monitor gradual processes in relatively little studied irrigated agricultural landscapes [5], where land degradation could be masked out due to the land management.

5. Conclusions

This study for the first time compared long-term (2003–2011) medium resolution vegetation index time series from the Medium Resolution Imaging Spectrometer (MERIS) and Moderate-resolution

Imaging Spectroradiometer (MODIS). This was done in the specific context of evaluation utility of the medium resolution image time series for detecting vegetation productivity decline in irrigated croplands. The study focused on the lower Amu Darya Basin in Uzbekistan in Central Asia. Vegetation Indices (VIs) derived from both MERIS and MODIS were useful in detecting negative vegetation trends, subject to some limitations. The estimated area of croplands with declined vegetation cover was generally larger based on MODIS than MERIS data and ranged in size from 22,472 ha (MERIS-MTCI) to 85,510 ha (MODIS-NDVI). NDVI (Normalized Differenced Vegetation Index) detected larger areas than SAVI (Soil-Adjusted Vegetation Index), while MTCI (MERIS Terrestrial Chlorophyll Index) identified the smallest areas affected by negative trends. For both MERIS- and MODIS-based trend analyses, SAVI time series identified an area of significant negative trends up to 1.5 times smaller than NDVI time series. SAVI has been found to be more appropriate for the detection of bare degraded soil patches in the study region.

Varying results of MERIS and MODIS are principally due to the different spectral and spatial characteristics of the sensors' data. Although MERIS has some spectral advantages, there is a need for more open access to these data and for higher processing levels for full resolution products including correction for angular effects. Development of user-friendly tools for preprocessing of this type of imagery will facilitate its usage. Aside from differences between sensors and indices, methodological challenges and limitations influence the results of trend analysis. Collecting field data to validate the results is recommendable to further assess the reliability of the remote sensing based maps independent of the sensor and VIs used. Nevertheless, the results of this study filled a knowledge gap on the differences in the results of trend analysis due to the choice of the medium resolution time series and indices for vegetation productivity decline monitoring.

Further analyses of the differences between MERIS and MODIS will be necessary to allow an effective fusion of the different datasets for the monitoring of vegetation dynamics over multi decade time periods. Great potential for further research exists to assess and evaluate data continuity issues, in particular those related to the scheduled launch of the Ocean and Land Color Instrument (OLCI) onboard the Sentinel-3 satellite.

Acknowledgments

The authors gratefully acknowledge the support of the Robert Bosch Foundation of Germany for supporting this study within the framework of the project "*Opportunities for Climate Change Mitigation Through Afforestation of Degraded Lands in Central Asia*". The authors are further thankful to ESA for furnishing the ENVISAT-MERIS data used in this study. These data were provided within the framework of the project "*Mapping Land Degradation Trends with Medium Spatial Resolution Optical Remote Sensing in Arid Irrigated Landscapes of Central Asia*" (Project ID 10447). We thank Guido Lüchters for his advice on statistical analyses. We are also grateful to Joseph Scepan of Medford, Oregon, USA, and three anonymous reviewers for their valuable comments.

Author Contributions

All authors contributed to the scientific content and authorship of this manuscript.

Conflicts of Interest

The authors declare no conflict of interest.

References

1. Sonnenschein, R.; Kuemmerle, T.; Udelhoven, T.; Stellmes, M.; Hostert, P. Differences in Landsat-based trend analyses in drylands due to the choice of vegetation estimate. *Remote Sens. Environ.* **2011**, *115*, 1408–1420.
2. Radke, R.J.; Andra, S.; Al-Kofahi, O.; Roysam, B. Image change detection algorithms: A systematic survey. *IEEE Trans. Image Process.* **2005**, *14*, 294–307.
3. Chen, G.; Hay, G.J.; Carvalho, L.M.T.; Wulder, M.A. Object-based change detection. *Int. J. Remote Sens.* **2012**, *33*, 4434–4457.
4. Li, X.-Y.; Ma, Y.-J.; Xu, H.-Y.; Wang, J.-H.; Zhang, D.-S. Impact of land use and land cover change on environmental degradation in lake Qinghai watershed, northeast Qinghai-Tibet Plateau. *Land Degrad. Dev.* **2009**, *20*, 69–83.
5. Gao, J.; Liu, Y. Determination of land degradation causes in Tongyu County, Northeast China via land cover change detection. *Int. J. Appl. Earth Obs. Geoinf.* **2010**, *12*, 9–16.
6. Yiran, G.A.B.; Kusimi, J.M.; Kufogbe, S.K. A synthesis of remote sensing and local knowledge approaches in land degradation assessment in the Bawku East District, Ghana. *Int. J. Appl. Earth Obs. Geoinf.* **2012**, *14*, 204–213.
7. Zanotta, D.C.; Haertel, V. Gradual land cover change detection based on multitemporal fraction images. *Pattern Recognit.* **2012**, *45*, 2927–2937.
8. Lambin, E.F.; Strahlers, A.H. Change-vector analysis in multitemporal space: A tool to detect and categorize land-cover change processes using high temporal-resolution satellite data. *Remote Sens. Environ.* **1994**, *48*, 231–244.
9. Zhao, G.X.; Lin, G.; Warner, T. Using Thematic Mapper data for change detection and sustainable use of cultivated land: A case study in the Yellow River delta, China. *Int. J. Remote Sens.* **2004**, *25*, 2509–2522.
10. Stellmes, M.; Udelhoven, T.; Röder, A.; Sonnenschein, R.; Hill, J. Dryland observation at local and regional scale—Comparison of Landsat TM/ETM+ and NOAA AVHRR time series. *Remote Sens. Environ.* **2010**, *114*, 2111–2125.
11. Wessels, K.J.; Prince, S.D.; Malherbe, J.; Small, J.; Frost, P.E.; VanZyl, D. Can human-induced land degradation be distinguished from the effects of rainfall variability? A case study in South Africa. *J. Arid Environ.* **2007**, *68*, 271–297.
12. Röder, A.; Udelhoven, T.; Hill, J.; del Barrio, G.; Tsiourlis, G. Trend analysis of Landsat-TM and -ETM+ imagery to monitor grazing impact in a rangeland ecosystem in Northern Greece. *Remote Sens. Environ.* **2008**, *112*, 2863–2875.
13. Dubovyk, O.; Menz, G.; Conrad, C.; Kan, E.; Machwitz, M.; Khamzina, A. Spatio-temporal analyses of cropland degradation in the irrigated lowlands of Uzbekistan using remote-sensing and logistic regression modeling. *Environ. Monit. Assess.* **2013**, *185*, 4775–4790.

14. Dubovyk, O.; Menz, G.; Khamzina, A. Trend Analysis of MODIS Time-Series Using Different Vegetation Indices for Monitoring of Cropland Degradation and Abandonment in Central Asia. In Proceedings of the 2012 IEEE International Geoscience and Remote Sensing Symposium (IGARSS), Munich, Germany, 22–27 July 2012; pp. 6589–6592.
15. Li, L.; Ustin, S.; Palacios-Orueta, A.; Jacquemoud, S.; Whiting, M. Remote Sensing Based Assessment of Biophysical Indicators for Land Degradation and Desertification. In *Recent Advances in Remote Sensing and Geoinformation Processing for Land Degradation Assessment*; Röder, A., Hill, J., Eds.; CRC Press: Boca Raton, FL, USA, 2009; pp. 15–44.
16. Tottrup, C.; Rasmussen, M.S. Mapping long-term changes in savannah crop productivity in Senegal through trend analysis of time series of remote sensing data. *Agric. Ecosyst. Environ.* **2004**, *103*, 545–560.
17. Huete, A.; Didan, K.; Miura, T.; Rodriguez, E.; Gao, X.; Ferreira, L. Overview of the radiometric and biophysical performance of the MODIS vegetation indices. *Remote Sens. Environ.* **2002**, *83*, 195–213.
18. Jeganathan, C.; Dash, J.; Atkinson, P.M. Mapping the phenology of natural vegetation in India using a remote sensing-derived chlorophyll index. *Int. J. Remote Sens.* **2010**, *31*, 5777–5796.
19. Diouf, A.; Lambin, E.F. Monitoring land-cover changes in semi-arid regions: Remote sensing data and field observations in the Ferlo, Senegal. *J. Arid Environ.* **2001**, *48*, 129–148.
20. Dash, J.; Curran, P.J. The MERIS terrestrial chlorophyll index. *Int. J. Remote Sens.* **2004**, *25*, 5403–5413.
21. Huete, A. A soil-adjusted vegetation index (SAVI). *Remote Sens. Environ.* **1988**, *25*, 295–309.
22. Fensholt, R.; Rasmussen, K.; Nielsen, T.T.; Mbow, C. Evaluation of earth observation based long term vegetation trends—Intercomparing NDVI time series trend analysis consistency of Sahel from AVHRR GIMMS, Terra MODIS and SPOT VGT data. *Remote Sens. Environ.* **2009**, *113*, 1886–1898.
23. Fensholt, R.; Proud, S.R. Evaluation of Earth Observation based global long term vegetation trends—Comparing GIMMS and MODIS global NDVI time series. *Remote Sens. Environ.* **2012**, *119*, 131–147.
24. Yin, H.; Udelhoven, T.; Fensholt, R.; Pflugmacher, D.; Hostert, P. How Normalized Difference Vegetation Index (NDVI) trendsfrom Advanced Very High Resolution Radiometer (AVHRR) and Système Probatoire d'Observation de la Terre VEGETATION (SPOT VGT) time series differ in agricultural areas: An Inner Mongolian case study. *Remote Sens.* **2012**, *4*, 3364–3389.
25. Si, Y.; Schlerf, M.; Zurita-Milla, R.; Skidmore, A.; Wang, T. Mapping spatio-temporal variation of grassland quantity and quality using MERIS data and the PROSAIL model. *Remote Sens. Environ.* **2012**, *121*, 415–425.
26. Zurita-Milla, R.; Clevers, J.G.P.W.; van Gijsel, J.A.E.; Schaepman, M.E. Using MERIS fused images for land-cover mapping and vegetation status assessment in heterogeneous landscapes. *Int. J. Remote Sens.* **2011**, *32*, 973–991.
27. Almond, S.; Boyd, D.S.; Dash, J.; Curran, P.J.; Hill, R.A.; Foody, G.M. Estimating Terrestrial Gross Primary Productivity with the Envisat Medium Resolution Imaging Spectrometer (MERIS) Terrestrial Chlorophyll Index (MTCI). In Proceedings of the 2010 IEEE International Geoscience and Remote Sensing Symposium (IGARSS), Honolulu, HI, USA, 25–30 July 2010; pp. 4792–4795.

28. Harris, A.; Dash, J. The potential of the MERIS Terrestrial Chlorophyll Index for carbon flux estimation. *Remote Sens. Environ.* **2010**, *114*, 1856–1862.
29. Boyd, D.S.; Almond, S.; Dash, J.; Curran, P.J.; Hill, R.A. Phenology of vegetation in Southern England from Envisat MERIS terrestrial chlorophyll index (MTCI) data. *Int. J. Remote Sens.* **2011**, *32*, 8421–8447.
30. Fensholt, R.; Sandholt, I.; Stisen, S. Evaluating MODIS, MERIS, and VEGETATION vegetation indices using *in situ* measurements in a semiarid environment. *IEEE Trans. Geosci. Remote Sens.* **2006**, *44*, 1774–1786.
31. Dash, J.; Jeganathan, C.; Atkinson, P.M. The use of MERIS Terrestrial Chlorophyll Index to study spatio-temporal variation in vegetation phenology over India. *Remote Sens. Environ.* **2010**, *114*, 1388–1402.
32. Dubovyk, O.; Menz, G.; Conrad, C.; Thonfeld, F.; Khamzina, A. Object-based identification of vegetation cover decline in irrigated agro-ecosystems in Uzbekistan. *Quat. Int.* **2013**, *311*, 163–174.
33. Dubovyk, O.; Menz, G.; Conrad, C.; Lamers, J.P. A.; Lee, A.; Khamzina, A. Spatial targeting of land rehabilitation: A relational analysis of cropland productivity decline in arid Uzbekistan. *Erdkunde* **2013**, *67*, 167–181.
34. Chub, E.V. *Climate Change and Its Impact on Natural Resources Potential of the Republic of Uzbekistan*; Central Asian Hydrometeorological Research Institute named after V.A. Bugayev: Tashkent, Uzbekistan, 2000.
35. UZSTAT. Crop Statistics for Khorezm Province 1998–2009. Unpublished work, 2010.
36. Djanibekov, N.; Rudenko, I.; Lamers, J.; Bobojonov, I. Pros and Cons of Cotton Production in Uzbekistan. In *Food Policy for Developing Countries: Food Production and Supply Policies*; Pinstrup-Andersen, P., Cheng, F., Eds.; Cornell University Press: Ithaca, NY, USA, 2010; pp. 13–27.
37. Ibrakhimov, M.; Khamzina, A.; Forkutsa, I.; Paluasheva, G.; Lamers, J.P.A.; Tischbein, B.; Vlek, P.L.G.; Martius, C. Groundwater table and salinity: Spatial and temporal distribution and influence on soil salinization in Khorezm region (Uzbekistan, Aral Sea Basin). *Irrig. Drain. Syst.* **2007**, *21*, 219–236.
38. Akramkhanov, A.; Martius, C.; Park, S.J.; Hendrickx, J.M.H. Environmental factors of spatial distribution of soil salinity on flat irrigated terrain. *Geoderma* **2011**, *163*, 55–62.
39. ESA. MERIS *Product Handbook. Issue 2.1*; European Space Agency: Frascati, Italy, 2006.
40. Vermote, E.F.; Kotchenova, S.Y.; Ray, J.P. *MODIS Surface Reflectance User's Guide*; MODIS Land Surface Reflectance Science Computing Facility: College Park, MD, USA, 2011.
41. Reynolds, J.F.; Smith, D.M.S.; Lambin, E.F.; Turner, B.L.; Mortimore, M.; Batterbury, S.P.J.; Downing, T.E.; Dowlatabadi, H.; Fernández, R.J.; Herrick, J.E.; *et al.* Global desertification: Building a science for dryland development. *Science* **2007**, *316*, 847–851.
42. Prince, S.D.; Becker-Reshef, I.; Rishmawi, K. Detection and mapping of long-term land degradation using local net production scaling: Application to Zimbabwe. *Remote Sens. Environ.* **2009**, *113*, 1046–1057.
43. Nicholson, S.E.; Tucker, C.J.; Ba, M.B. Desertification, drought, and surface vegetation: An example from the West African Sahel. *Bull. Am. Meteorol. Soc.* **1998**, *79*, 815–829.

44. Wessels, K.J.; Prince, S.D.; Frost, P.E.; van Zyl, D. Assessing the effects of human-induced land degradation in the former homelands of northern South Africa with a 1 km AVHRR NDVI time-series. *Remote Sens. Environ.* **2004**, *91*, 47–67.
45. Akramkhanov, A.; Kuziev, R.; Sommer, R.; Martius, C.; Forkutsa, O.; Massucati, L. Soils and Soil Ecology in Khorezm. In *Cotton, Water, Salts and Soums*; Martius, C., Rudenko, I., Lamers, J.P.A., Vlek, P.L.G., Eds.; Springer: Dordrecht, The Netherlands, 2012; pp. 37–58.
46. Clevers, J.G.P.W.; Schaepman, M.E.; Mücher, C.A.; de Wit, A.J.W.; Zurita-Milla, R.; Bartholomeus, H.M. Using MERIS on Envisat for land cover mapping in the Netherlands. *Int. J. Remote Sens.* **2007**, *28*, 637–652.
47. Gitelson, A.A.; Viña, A.; Verma, S.B.; Rundquist, D.C.; Arkebauer, T.J.; Keydan, G.; Leavitt, B.; Ciganda, V.; Burba, G.G.; Suyker, A.E. Relationship between gross primary production and chlorophyll content in crops: Implications for the synoptic monitoring of vegetation productivity. *J. Geophys. Res.* **2006**, *111*, doi:10.1029/2005JD006017.
48. Rouse, J.; Haas, R.; Schell, J. *Monitoring the Vernal Advancement and Retrogradation (Greenwave Effect) of Natural Vegetation*; Texas A and M University: College Station, TX, USA, 1974.
49. Le, Q.B.; Tamene, L.; Vlek, P.L.G. Multi-pronged assessment of land degradation in West Africa to assess the importance of atmospheric fertilization in masking the processes involved. *Glob. Planet. Chang.* **2012**, *92–93*, 71–81.
50. Huete, A.R.; Jackson, R.D.; Post, D.F. Spectral response of a plant canopy with different soil backgrounds. *Remote Sens. Environ.* **1985**, *17*, 37–53.
51. Gomez-Chova, L.; Zurita-Milla, R.; Alonso, L.; Amoros-Lopez, J.; Guanter, L.; Camps-Valls, G. Gridding artifacts on medium-resolution satellite image time series: MERIS case study. *IEEE Trans. Geosci. Remote Sens.* **2011**, *49*, 2601–2611.
52. Holben, B.N. Characteristics of maximum-value composite images from temporal AVHRR data. *Int. J. Remote Sens.* **1986**, *7*, 1417–1434.
53. Dash, J.; Lankester, T.; Hubbard, S.; Curran, P.J. Signal-to-Noise Ratio for MTCI and NDVI Time Series Data. In Proceedings of the 2nd MERIS/(A)ATSR User Workshop, Rome, Italy, 22–26 September 2008.
54. Wessels, K.J.; Prince, S.D.; Reshef, I. Mapping land degradation by comparison of vegetation production to spatially derived estimates of potential production. *J. Arid Environ.* **2008**, *72*, 1940–1949.
55. Mann, H.B. Nonparametric tests against trend. *Econometrica* **1945**, *13*, 245–259.
56. Kendall, M.G. A new measure of rank correlation. *Biometrika* **1938**, *30*, 81–93.
57. De Jong, R.; de Bruin, S.; de Wit, A.; Schaepman, M.E.; Dent, D.L. Analysis of monotonic greening and browning trends from global NDVI time-series. *Remote Sens. Environ.* **2011**, *115*, 692–702.
58. Wessels, K.J.; van den Bergh, F.; Scholes, R.J. Limits to detectability of land degradation by trend analysis of vegetation index data. *Remote Sens. Environ.* **2012**, *125*, 10–22.
59. Shoji, T.; Kitaura, H. Statistical and geostatistical analysis of rainfall in central Japan. *Comput. Geosci.* **2006**, *32*, 1007–1024.

60. Bland, J.M.; Altman, D.G. Statistical methods for assessing agreement between two methods of clinical measurement. *Lancet* **1986**, *327*, 307–310.
61. Bréon, F.-M.; Vermote, E. Correction of MODIS surface reflectance time series for BRDF effects. *Remote Sens. Environ.* **2012**, *125*, 1–9.
62. Curran, P.J.; Dash, J. [Report on] Algorithm Theoretical Basis Document: Chlorophyll Index. Available online: http://www.esa.int (accessed on 4 Auguest 2013).
63. Slay, B.; Juraev, A. *The Return of Drought Conditions to Central Asia: Update and Possible Impact on Food Security ("Fast Facts" from Central Asia's Reservoirs, and Official Socio-Economic Data)*; UNDP Regional Bureau for Europe and CIS: Bratislava, Slovakia, 2011.
64. Thenkabail, P.S.; Smith, R.B.; de Pauw, E. Hyperspectral vegetation indices and their relationships with agricultural crop characteristics. *Remote Sens. Environ.* **2000**, *71*, 158–182.
65. Curran, P.J.; Steele, C.M. MERIS: The re-branding of an ocean sensor. *Int. J. Remote Sens.* **2005**, *26*, 1781–1798.
66. Jackson, R.D.; Huete, A.R. Interpreting vegetation indices. *Prev. Vet. Med.* **1991**, *11*, 185–200.
67. Fensholt, R.; Langanke, T.; Rasmussen, K.; Reenberg, A.; Prince, S.D.; Tucker, C.; Scholes, R.J.; Le, Q.B.; Bondeau, A.; Eastman, R.; *et al.* Greenness in semi-arid areas across the globe 1981–2007—An Earth Observing Satellite based analysis of trends and drivers. *Remote Sens. Environ.* **2012**, *121*, 144–158.